Front. Phys. 12(3), 127501 (2017)
DOI 10.1007/s11467-017-0653-2

RESEARCH ARTICLE

# Multiple conical spin order in spinel structure stabilized by magnetic anisotropy

**Xiao-Yan Yao**[1,†], **Li-Juan Yang**[2]

[1] *Department of Physics, Southeast University, Nanjing* 211189, *China*
[2] *School of Information Science and Technology, Suqian College, Suqian* 223800, *China*
*Corresponding author. E-mail:* [†] *yaoxiaoyan@seu.edu.cn*
*Received October 31, 2016; accepted December 21, 2016*

Conical spin order, where the spin components along the conical axis form magnetization while the spiral parts induce ferroelectric polarization, possesses multiferroicity with inherent magnetoelectric coupling. A Monte Carlo simulation performed using a classical Heisenberg spinel ($AB_2O_4$) model reveals a multiple conical spin order, i.e., three modulations with different cone angles and wavelengths on A sites and two alternate B sites. The spin order not only exists as the ground state but also survives locally stably in a larger parameter region. The whole existence range can be effectively expanded by anisotropy to cover the cases of $CoCr_2O_4$ and $MnCr_2O_4$. The multiple conical spin order is well maintained and finely tuned by frustration and anisotropy over the whole existence range, and the magnetic and ferroelectric properties are influenced correspondingly.

**Keywords** conical spin order, multiferroicity, spinel structure, Monte Carlo simulation

**PACS numbers** 75.25.-j, 75.85.+t, 75.50.Gg



## 1 Introduction

Conical spin order provides a special realization of multiferroicity, where a net magnetization is formed by the spin components along the conical axis, while the spiral parts induce ferroelectric polarization in the spiral plane. This conical magnetism-driven multiferroicity was first observed in the spinel compound $CoCr_2O_4$ [1–3], where the conical spin order is inherent and stable even without magnetic field. Later, the intrinsic or magnetic field-induced conical spin structure was found to play essential roles in the multiferroic behaviors of many other materials [4–8]. In particular, the attractive low-field magnetoelectric effect at room temperature, observed in Z-type and M-type hexaferrites, originates from the conical spin structure [9–11]. The magnetic origin of ferroelectricity in the conical spin order determines the inherent magnetoelectric coupling, which is advantageous for realizing various mutual controls between magnetism and ferroelectricity [1, 12–16].

The cubic spinel structure with the general formula $AB_2O_4$ (Fig. 1) is a basic structure for realizing the intrinsic conical spin order. It was suggested by Lyons, Kaplan, Dwight, and Menyuk (LKDM) that the conical spin order has the lowest energy among a large set of possible spin configurations in the spinel structure under the condition that $8/9 < u < 1.298$, where $u = 4j_{BB}s_B/(3j_{AB}s_A)$ [17, 18]. $s_A$ and $s_B$ are the spin magnitudes at the A and B sites, respectively, and only the nearest-neighboring antiferromagnetic A-B ($j_{AB}$) and B-B ($j_{BB}$) exchange interactions are considered. However, the $u$ values obtained by fitting the experimental data to the theoretical spin structure are approximately 2.0 for $CoCr_2O_4$ and 1.6 or 1.5 for $MnCr_2O_4$ [19–21]. These values are beyond the $u$-range of the conical spin order predicted by the LKDM theory. Various efforts have been directed towards solving this puzzle [22, 23]. Our previous work revealed that anisotropy played an important role in stabilizing the conical spin order [24]. Because anisotropy always exists in these compounds with conical spin order [1, 3, 21], further studies on the conical spin order under the influence of anisotropy are required. In the present study, a simulation presents in detail a multiple conical spin order, revealing three modulations with different cone angles and wavelengths on A sites and two alternate B sites in the spinel lattice, which not only exists as the ground state but also survives locally stably over a larger parameter region. Its whole existence range can be effectively expanded by anisotropy, where

© Higher Education Press and Springer-Verlag Berlin Heidelberg 2017

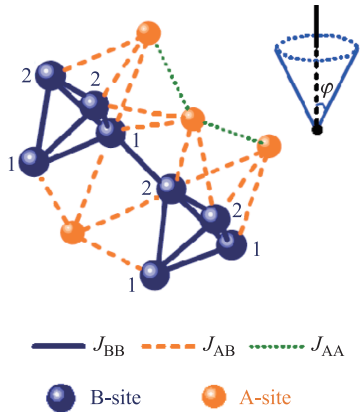


**Fig. 1** A sketch of spinel structure (half-cubic unit cell) with A and B sites as well as $J_{BB}$, $J_{AB}$ and $J_{AA}$. Here 1 and 2 mark B sites on the alternate layers along $z$-axis. The cone angle $\varphi$ is illustrated in the inset.

the conical spin order is well maintained and finely tuned by anisotropy and frustration, which correspondingly influences the magnetic and ferroelectric properties.

## 2 Model and simulation

Considering the relatively nearest-neighboring antiferromagnetic A-B and B-B exchange interactions as $J_{BB} = j_{BB}s_B s_B$ and $J_{AB} = j_{AB}s_A s_B$, the Hamiltonian is written as

$$H = J_{BB}\sum_{[i,j]} \boldsymbol{S}_{Bi}\cdot\boldsymbol{S}_{Bj} + J_{AB}\sum_{[i,j]} \boldsymbol{S}_{Ai}\cdot\boldsymbol{S}_{Bj} - K\sum_i[(S^z_{Bi})^2 + (S^z_{Ai})^2]. \quad (1)$$

Here $S_{Bi}$ and $S_{Ai}$ are the $i^{\text{th}}$ normalized classic spins on the B and A sites of the spinel lattice, and $[i,j]$ denotes the summation over all the nearest-neighboring spin pairs. The third term on the right side of Eq. (1) is the energy of single-ion anisotropy along the $z$-axis with strength $K$. For convenience, $J_{AB}$ is chosen to be unity, and the other parameters are scaled accordingly.

A Monte Carlo simulation is performed for a three-dimensional (3D) spinel lattice with classical Heisenberg spins using the Metropolis algorithm with periodic boundary conditions applied. Systems of different sizes are calculated to confirm that the lattice size does not influence the main results, and the effects of the lattice size on the detailed magnetic structure are examined. To explore the ground state at every parameter point, the system is subjected to a gradual cooling procedure under weak poling electric and magnetic fields, and then the minimization algorithm for the energy without external fields is applied to further push the system to the limit of zero temperature. The ground state is estimated by comparing states evolved from different initial states under poling fields of different magnitudes. The local stability, i.e., the stability against arbitrary small deviations of all the spin vectors from their original directions, is confirmed if the conical spin structure can survive the thermal fluctuation of $T = 0.01$.

## 3 Results and discussion

In the spinel structure $AB_2O_4$, B sites are arranged in a pyrochlore sub-lattice, and A sites form a diamond sub-lattice. When A and B sites are both occupied by magnetic ions, the exchange interactions between them compete with each other, providing a particular condition to form an inherent conical spin order. The simulation presents a multiple conical spin order, as shown in Fig. 2, with $J_{BB} = 0.833\,33$ and $K = 0$ in the parameter range given by the LKDM theory. As illustrated in Fig. 2(a), three modulations emerge on A sites and two different B sites: B1 and B2, as marked in Fig. 1. If the sites of all the spins are moved to zero, three different spin cones, i.e., the surface of the cone on which the spin vectors lie, are formed by the spins on the B1, B2, and A sites [Fig. 2(d)]. The orientation of the B1 cone is parallel to the B2 cone and antiparallel to the A cone. All the three conical spin orders are aligned in the same direction $k$, and $k$ can be any one of twelve symmetric $\langle 110\rangle$ directions. To clarify the spin configuration in detail, one layer of B2-site spins is plotted in Fig. 2(b), and one layer of spins on B1 and A sites is illustrated in Fig. 2(c). Perfect spiral components of spins are observed along $k$, and different wavelengths are observed on the three sites. Furthermore, snapshots along $k$ and $k'$ (the direction perpendicular to $k$ on the spiral plane) are presented in Figs. 2(e) and (f), where B1 and B2 layers are alternately stacked with A sites inserted between them. The spins on the lines along $k'$ overlap completely with each other, while the spins on the lines along $k$ show different orientations, that is, a conical modulation along $k$. To characterize this multiple conical spin order effectively, the average cone angle ($\varphi$ as illustrated in Fig. 1) is calculated for spins on B1, B2, and A sites — $\varphi_{B1}$, $\varphi_{B2}$, and $\varphi_A$, respectively — which can also be used to distinguish other states.

To observe the ground states under the influence of anisotropy, $\varphi_{B1}$, $\varphi_{B2}$, and $\varphi_A$ are evaluated as functions of $J_{BB}$ for different $K$ values, as shown in Figs. 3(a)–(e). For $K = 0$–$0.4$, as $J_{BB}$ increases, four phases are distinguished by the feature of the cone angles. The first is the Neel (N) phase with the typical spin configuration shown in Fig. 3(f), where $\varphi_{B1} = \varphi_{B2} = 180°$ and $\varphi_A = 0$ with nearly no error bar. In this phase, all the A-site spins are parallel to each other and antiparallel to all

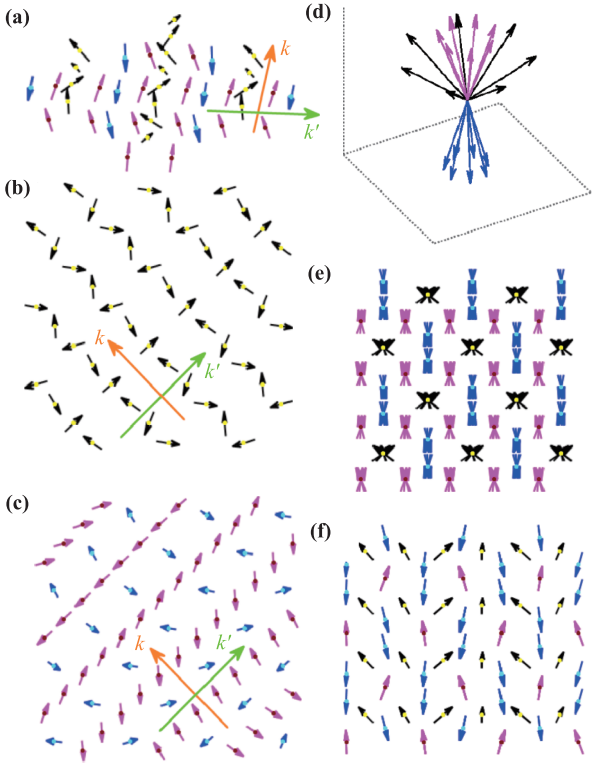


**Fig. 2** The detailed spin configuration with $J_{BB} = 0.83333$ and $K = 0$. The pink, black and blue arrows show spin vectors on B1, B2 and A sites, where the site locations are marked by small dots. $k$ denotes the direction of conical modulation, while $k'$ marks the direction perpendicular to $k$ on the spiral plane. **(a)** The snapshot for partial spin configuration with one layer of B1-site spins, one layer of B2-site spins and one layer A-site spins together. **(b)** One layer of spins on B2 sites, where the arrows show the projections of spins onto spiral plane. **(c)** One layer of B1-site spins and one layer of A-site spins, where the arrows show the projections of spins onto spiral plane, which are magnified by 3.2 to present an appropriate magnitude. **(d)** If sites of all the spins are moved to zero, then the spin vectors on B1, B2 and A sites respectively lie on the surfaces of three different cones. **(e)** The snapshot viewed along $k$. **(f)** The snapshot viewed along $k'$.

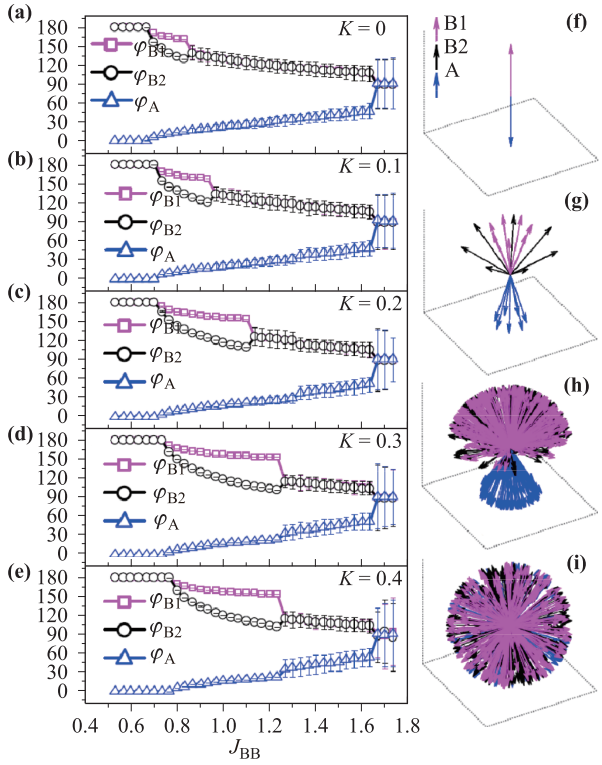


**Fig. 3** **(a–e)** The averaged cone angles of spins on A sites ($\varphi_A$) and two B sites ($\varphi_{B1}$ and $\varphi_{B2}$) as functions of $J_{BB}$ at different $K$ from 0 to 0.4. The typical spin configurations with their sites moved to zero are plotted for **(f)** N, **(g)** C, **(h)** F and **(i)** D phases. The pink, black and blue arrows show spin vectors on B1, B2 and A sites.

the B-site spins. The second is the Conical (C) phase, which is characterized by three different values for $\varphi_A$, $\varphi_{B1}$, and $\varphi_{B2}$ with very small error bars, corresponding to three perfect spin cones formed by spins on B1, B2, and A sites, respectively, as illustrated in Fig. 3(g). The third is the Ferrimagnetic (F) phase with the typical spin configuration shown in Fig. 3(h), where $\varphi_{B1} \approx \varphi_{B2} \neq \varphi_A$ with obvious error bars. This is a complex state with mixed modulations. The fourth is the Disordered (D) phase, as plotted in Fig. 3(i) with $\varphi_{B1} \approx \varphi_{B2} \approx \varphi_A \approx 90$ and very large error bars. The anisotropy has obvious effects on the F and C phases: the C phase is well stabilized in a larger $J_{BB}$ range and moves slightly to a higher $J_{BB}$, while the F phase is suppressed. The magnetic phase diagram in the parameter space of $K$ and $J_{BB}$ is summarized in Fig. 4(a), where the whole parameter space is divided into four main parts: N, C, F, and D.

Notably, the multiple conical spin order not only exists as the ground state but also can be locally stable over a larger parameter range in the spinel structure [18, 24]. In Fig. 4(a), its locally stable range is plotted as the shaded area, appearing immediately above the region of the ground-state C phase. Figures 4(b)–(d) show $\varphi_A$, $\varphi_{B1}$, and $\varphi_{B2}$ calculated for the whole existence range, including the ground state and the locally stable parts. In the case of $K = 0$, the conical spin order exists in the range of $J_{BB} = 0.666\ 67$ to $0.9667$, which agrees well with the LKDM theory [18]. Although the spin cone is slightly compressed, the anisotropy can locally stabilize the conical spin order very effectively. In particular, the multiple conical spin order is maintained to $J_{BB} = 1.2$ with $K \geq 0.2$ and $J_{BB} = 1.5$ with $K \geq 0.4$, which correspond to $u = 1.6$ in $MnCr_2O_4$ and $u = 2.0$ in $CoCr_2O_4$. When $J_{BB} = 1.2$, $\varphi_A = 24.11°$, $23.22°$, and $22.35°$; $\varphi_{B1} = 152.69°$, $153.36°$, and $153.98°$; and

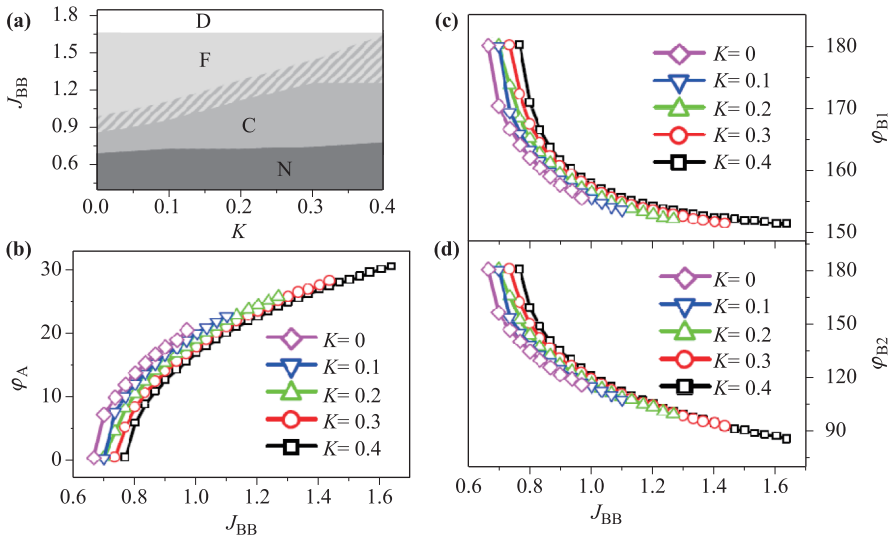


**Fig. 4** **(a)** The simulated magnetic phase diagram on the parameter space of $J_{BB}$ and $K$, which is divided into four parts, namely N, C, F, and D phases. The shaded region above C phase shows the locally stable range of multiple conical spin order. **(b)** $\varphi_A$, **(c)** $\varphi_{B1}$, and **(d)** $\varphi_{B2}$ as functions of $J_{BB}$ at different $K$ from 0 to 0.4, which are calculated on the whole existence range of conical spin order, including ground state and locally stable parts.

$\varphi_{B2} = 102.71°$, $103.53°$, and $104.43°$ for $K = 0.2$, 0.3, and 0.4, respectively, which is well consistent with a previous report regarding $MnCr_2O_4$ ($\varphi_A = 24°$, $\varphi_{B1} = 152°$, and $\varphi_{B2} = 104°$) [19]. When $J_{BB} = 1.5$ and $K = 0.4$, $\varphi_A = 28.23°$, $\varphi_{B1} = 151.77°$, and $\varphi_{B2} = 90°$, which is consistent with a previous report regarding $CoCr_2O_4$ ($\varphi_A = 32°$, $\varphi_{B1} = 150°$, $\varphi_{B2} = 90°$) [20]. In addition, at $K = 0.4$, $\varphi_{B2}$ crosses 90° at approximately $J_{BB} = 1.5$, i.e., the flipping of B2 spin cone, and then the B1 and B2 spin cones show opposite orientations, which is similar to another possibility discussed for $CoCr_2O_4$ [21]. Therefore, the anisotropy can be a very important factor for stabilizing the conical spin order at the large $u$ values expected in real materials. Because $u$ indicates the competition between B-B coupling and B-A coupling, a large $u$ indicates a relatively strong frustration.

The multiple conical spin order is well maintained over the whole existence range, as confirmed in Figs. 4(b)–(d). The three conical modulations show different wavelengths on B1, B2, and A sites, which are defined as $\lambda_{B1}$, $\lambda_{B2}$, and $\lambda_A$ in units of the distance between two nearest-neighboring B sites. The simulation always shows $\lambda_{B1} = \lambda_A \neq \lambda_{B2}$, and the values are approximately incommensurate with the lattice periodicity. These wavelengths are sensitive to the lattice size ($L \times L \times L$) because of the periodic boundary conditions. For example, when $K = 0.2$ and $J_{BB} = 1.2$ are fixed, if $L = 52$, $\lambda_{B1} = \lambda_A = 5.200$ and $\lambda_{B2} = 3.250$, but if $L = 36$, $\lambda_{B1} = \lambda_A = 4.500$ and $\lambda_{B2} = 3.600$. To overcome the effect of the boundary conditions, lattices of different sizes ($L = 20-76$) are simulated to obtain conical spin structures with different wavelengths. Figure 5(a) presents the energy ($E$) as a function of the ratio of $\lambda_{B2}$ to $\lambda_{B1}$. We observe that the minimum of $E$ appears around $\lambda_{B2}/\lambda_{B1} = 0.7$, where $\lambda_{B1} = \lambda_A = 4.857$ and $\lambda_{B2} = 3.400$, which could be the optimal ratio for the multiple conical spin order in the case of $K = 0.2$ and $J_{BB} = 1.2$. This optimal ratio is not very sensitive to $J_{BB}$. When $K$ is increased, the optimal ratio decreases slightly. The effect of $\lambda_{B2}/\lambda_{B1}$ on the spin configuration is shown in Figs. 5(b)–(d). Here, we observe that as $\lambda_{B2}/\lambda_{B1}$ increases, $\varphi_{B1}$ and $\varphi_{B2}$ decrease, but $\varphi_A$ increases.

According to the spin configuration, the multiferroic properties of the multiple conical spin order are evaluated over its existence range, as shown in Fig. 6. The magnetization ($M$) is evaluated as

$$\boldsymbol{M} = \sum_i (\boldsymbol{S}_{Ai} + \boldsymbol{S}_{Bi}). \tag{2}$$

The orientation of $M$ is along the $z$-axis, i.e., perpendicular to the spiral plane formed by $k$ and $k'$. The magnitude of $M$ ($|M|$) decreases as $J_{BB}$ increases, as plotted in Fig. 6(a). When the B2 spin cone flips at approximately $J_{BB} = 1.5$ with $K = 0.4$, $M$ also changes its sign. The ferroelectric polarization ($P$) is calculated according to the spin-current model and the theory of inverse Dzyaloshinskii–Moriya interaction [25, 26]:

$$\boldsymbol{P} = -\sum_{[i,j]} \boldsymbol{e}_{ij} \times (\boldsymbol{S}_i \times \boldsymbol{S}_j), \tag{3}$$

where $e_{ij}$ denotes the vector connecting the neighboring $S_i$ and $S_j$. For convenience, only the spin current between the spins of the B site is considered in the poling

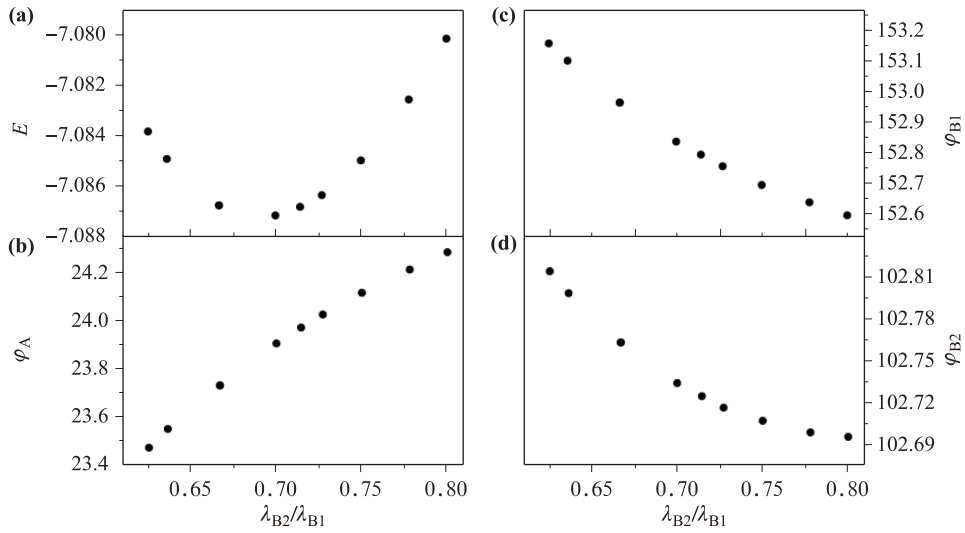


**Fig. 5** **(a)** The energy ($E$), **(b)** $\varphi_{\rm A}$, **(c)** $\varphi_{\rm B1}$, and **(d)** $\varphi_{\rm B2}$ as functions of $\lambda_{\rm B2}/\lambda_{\rm B1}$ at $K = 0.2$ and $J_{BB} = 1.2$.

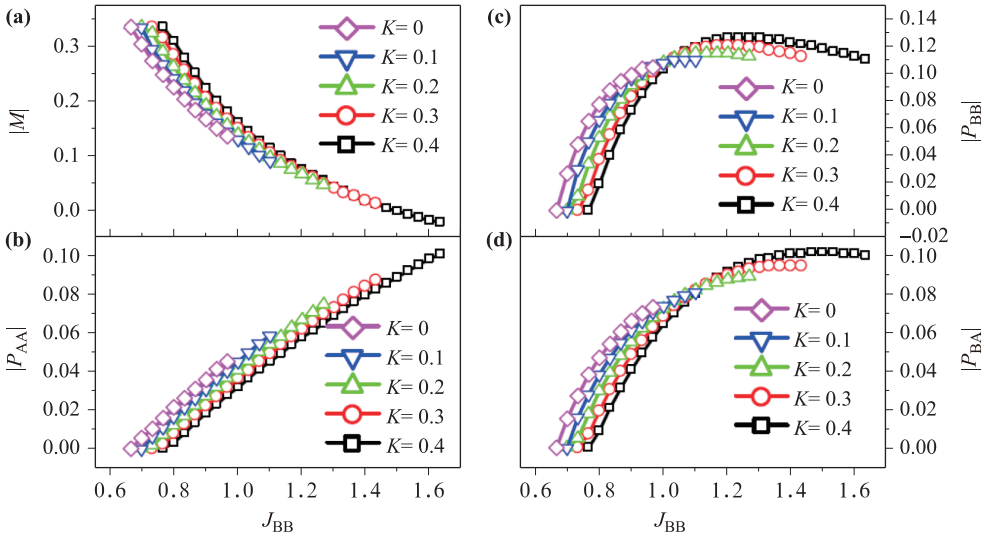


**Fig. 6** The absolute value of magnetization **(a)** $|M|$, the absolute values of ferroelectric polarizations **(b)** $|P_{\rm AA}|$, **(c)** $|P_{\rm BB}|$ and **(d)** $|P_{\rm BA}|$ as functions of $J_{\rm BB}$ for different $K = 0{-}0.4$ on the existence range of conical spin order, including ground state and locally stable parts.

procedure. Because different conical modulations coexist at different sites, ferroelectricity can occur not only on B-B bonds but also on other bonds. $P_{\rm AA}$, $P_{\rm BB}$, and $P_{\rm BA}$ — calculated for A-A, B-B, and B-A bonds, respectively — are all aligned along the $k'$ direction, but $P_{\rm BB}$ and $P_{\rm AA}$ have an orientation opposite to that of $P_{\rm BA}$. Figures 6(b)–(d) plot their magnitudes as functions of $J_{\rm BB}$ with $K = 0{-}0.4$. As $J_{\rm BB}$ increases, $|P_{\rm AA}|$ increases monotonously. $|P_{\rm BB}|$ and $|P_{\rm BA}|$ also increase but gradually form a broad peak as $K$ increases, and the maximum of $|P_{\rm BB}|$ is located at a $J_{\rm BB}$ smaller than that for $|P_{\rm BA}|$. The different behaviors suggest the possibility of producing a complex ferroelectric phenomenon in experiments [3].

## 4 Conclusion

Monte Carlo simulation is performed using a 3D classical Heisenberg model to investigate the multiferroic conical spin order in a spinel lattice. It is confirmed that the existence range of the conical spin order, including the ground state and locally stable parts, can be effectively expanded by anisotropy up to cover the cases of $CoCr_2O_4$

and $MnCr_2O_4$. The multiple conical spin order shows three modulations with different cone angles and wavelengths emerging on A sites and two alternate B sites and is well maintained and finely tuned by frustration and anisotropy over the whole existence range, which correspondingly influences the magnetic and ferroelectric properties. Because the spinel blocks, which always exist in Y-, M-, and Z-type hexaferrites, are observed to play an essential role in producing the magnetoelectric conical spin structure [27, 28], our results will help to clarify the conical magnetism and the corresponding multiferroicity in additional materials.

**Acknowledgements** This work was supported by the research grants from the Natural Science Foundation of Jiangsu Province of China (Grant Nos. BK20141329 and 15KJB140009).



## References


1. Y. Yamasaki, S. Miyasaka, Y. Kaneko, J. P. He, T. Arima, and Y. Tokura, Magnetic reversal of the ferroelectric polarization in a multiferroic spinel oxide, *Phys. Rev. Lett.* 96(20), 207204 (2006)
2. I. Kim, Y. S. Oh, Y. Liu, S. H. Chun, J. S. Lee, K. T. Ko, J. H. Park, J. H. Chung, and K. H. Kim, Electric polarization enhancement in multiferroic $CoCr_2O_4$ crystals with Cr-site mixing, *Appl. Phys. Lett.* 94(4), 042505 (2009)
3. Y. J. Choi, J. Okamoto, D. J. Huang, K. S. Chao, H. J. Lin, C. T. Chen, M. van Veenendaal, T. A. Kaplan, and S. W. Cheong, Thermally or magnetically induced polarization reversal in the multiferroic $CoCr_2O_4$, *Phys. Rev. Lett.* 102(6), 067601 (2009)
4. I. Urcelay-Olabarria, E. Ressouche, A. A. Mukhin, V. Y. Ivanov, A. M. Balbashov, J. L. Garcia-Munoz, and V. Skumryev, Conical antiferromagnetic order in the ferroelectric phase of $Mn_{0.8}Co_{0.2}WO_4$ resulting from the competition between collinear and cycloidal structures, *Phys. Rev. B* 85(22), 224419 (2012)
5. N. Kida, D. Okuyama, S. Ishiwata, Y. Taguchi, R. Shimano, K. Iwasa, T. Arima, and Y. Tokura, Electric-dipole-active magnetic resonance in the conical-spin magnet $Ba_2Mg_2Fe_{12}O_{22}$, *Phys. Rev. B* 80(22), 220406 (2009)
6. S. Ishiwata, Y. Taguchi, Y. Tokunaga, H. Murakawa, Y. Onose, and Y. Tokura, Electric polarization induced by transverse magnetic field in the anisotropy-controlled conical helimagnet $Ba_2(Mg_{1-x}Zn_x)_2Fe_{12}O_{22}$, *Phys. Rev. B* 79(18), 180408 (2009)
7. H. B. Lee, S. H. Chun, K. W. Shin, B. G. Jeon, Y. S. Chai, K. H. Kim, J. Schefer, H. Chang, S. N. Yun, T. Y. Joung, and J. H. Chung, Heliconical magnetic order and field-induced multiferroicity of the $Co_2Y$-type hexaferrite $Ba_{0.3}Sr_{1.7}Co_2Fe_{12}O_{22}$, *Phys. Rev. B* 86(9), 094435 (2012)
8. L. Lin, H. X. Zhu, X. M. Jiang, K. F. Wang, S. Dong, Z. B. Yan, Z. R. Yang, J. G. Wan, and J. M. Liu, Coupled ferroelectric polarization and magnetization in spinel $FeCr_2S_4$, *Sci. Rep.* 4, 6530 (2014)
9. Y. Kitagawa, Y. Hiraoka, T. Honda, T. Ishikura, H. Nakamura, and T. Kimura, Low-field magnetoelectric effect at room temperature, *Nat. Mater.* 9(10), 797 (2010)
10. Y. Tokunaga, Y. Kaneko, D. Okuyama, S. Ishiwata, T. Arima, S. Wakimoto, K. Kakurai, Y. Taguchi, and Y. Tokura, Multiferroic M-type hexaferrites with a room-temperature conical state and magnetically controllable spin helicity, *Phys. Rev. Lett.* 105(25), 257201 (2010)
11. M. Soda, T. Ishikura, H. Nakamura, Y. Wakabayashi, and T. Kimura, Magnetic ordering in relation to the room-temperature magnetoelectric effect of $Sr_3Co_2Fe_{24}O_{41}$, *Phys. Rev. Lett.* 106(8), 087201 (2011)
12. S. Ishiwata, Y. Taguchi, H. Murakawa, Y. Onose, and Y. Tokura, Low-magnetic-field control of electric polarization vector in a helimagnet, *Science* 319(5870), 1643 (2008)
13. H. Murakawa, Y. Onose, K. Ohgushi, S. Ishiwata, and Y. Tokura, Generation of electric polarization with rotating magnetic field in helimagnet $ZnCr_2Se_4$, *J. Phys. Soc. Jpn.* 77(4), 043709 (2008)
14. H. Murakawa, Y. Onose, F. Kagawa, S. Ishiwata, Y. Kaneko, and Y. Tokura, Rotation of an electric polarization vector by rotating magnetic field in cycloidal magnet $Eu_{0.55}Y_{0.45}MnO_3$, *Phys. Rev. Lett.* 101(19), 197207 (2008)
15. X. Yao, V. C. Lo, and J. M. Liu, Magnetic field controlled reversal of ferroelectric polarization in conical spin ordered multiferroics: Monte Carlo simulation, *J. Appl. Phys.* 106(7), 073901 (2009)
16. X. Yao, Continuous rotation of magnetization controlled by electric field in multiferroic state originated from conical spin order, *J. Phys. Soc. Jpn.* 79(4), 043801 (2010)
17. T. A. Kaplan, K. Dwight, D. Lyons, and N. Menyuk, Classical theory of the ground spin state in spinels, *J. Appl. Phys.* 32(3), S13 (1961)
18. D. H. Lyons, T. A. Kaplan, K. Dwight, and N. Menyuk, Classical theory of the ground spin-state in cubic spinels, *Phys. Rev.* 126(2), 540 (1962)
19. J. M. Hastings and L. M. Corliss, Magnetic structure of manganese chromite, *Phys. Rev.* 126(2), 556 (1962)
20. N. Menyuk, K. Dwight, and A. Wold, Ferrimagnetic spiral configurations in cobalt chromite, *J. Phys. (Paris)* 25(5), 528 (1964)
21. K. Tomiyasu, J. Fukunaga, and H. Suzuki, Magnetic short-range order and reentrant-spin-glass-like behavior in $CoCr_2O_4$ and $MnCr_2O_4$ by means of neutron scattering and magnetization measurements, *Phys. Rev. B* 70(21), 214434 (2004)

22. C. Ederer and M. Komelj, Magnetic coupling in $CoCr_2O_4$ and $MnCr_2O_4$: An LSDA + $U$ study, *Phys. Rev. B* 76(6), 064409 (2007)
23. G. Lawes, B. Melot, K. Page, C. Ederer, M. A. Hayward, T. Proffen, and R. Seshadri, Dielectric anomalies and spiral magnetic order in $CoCr_2O_4$, *Phys. Rev. B* 74(2), 024413 (2006)
24. X. Yao, Stable and locally stable conditions for a conical spin state in the spinel structure, *EPL* 102(6), 67013 (2013)
25. H. Katsura, N. Nagaosa, and A. V. Balatsky, Spin current and magnetoelectric effect in noncollinear magnets, *Phys. Rev. Lett.* 95(5), 057205 (2005)
26. I. A. Sergienko and E. Dagotto, Role of the Dzyaloshinskii–Moriya interaction in multiferroic perovskites, *Phys. Rev. B* 73(9), 094434 (2006)
27. H. Sagayama, K. Taniguchi, N. Abe, T. Arima, Y. Nishikawa, S. I. Yano, Y. Kousaka, J. Akimitsu, M. Matsuura, and K. Hirota, Two distinct ferroelectric phases in the multiferroic Y-type hexaferrite $Ba_2Mg_2Fe_{12}O_{22}$, *Phys. Rev. B* 80(18), 180419 (2009)
28. S. P. Shen, Y. S. Chai, J. Z. Cong, P. J. Sun, J. Lu, L. Q. Yan, S. G. Wang, and Y. Sun, Magnetic-ion-induced displacive electric polarization in $FeO_5$ bipyramidal units of (Ba, Sr)$Fe_{12}O_{19}$ hexaferrites, *Phys. Rev. B* 90(18), 180404(R) (2014)